

# Direct-current control of radiation-induced differential magnetoresistance oscillations in two-dimensional electron systems

X. L. Lei

*Department of Physics, Shanghai Jiaotong University, 1954 Huashan Road, Shanghai 200030, China*

Magnetoresistance oscillations in two-dimensional electron systems driven simultaneously by a strong direct current and a microwave irradiation, are analyzed within a unified microscopic scheme treating both excitations on an equal footing. The microwave-induced resistance oscillations are described by a parameter  $\epsilon_\omega$  proportional to the radiation frequency, while the dc-induced resistance oscillations are governed by a parameter  $\epsilon_j$  proportional to the current density. In the presence of both a microwave radiation and a strong dc, the combined parameter  $\epsilon_\omega + \epsilon_j$  is shown to control the main resistance oscillations, in agreement with the recent measurement [Zhang *et al.* Phys. Rev. Lett. **98**, 106804 (2007)].

PACS numbers: 73.50.Jt, 73.40.-c, 73.43.Qt, 71.70.Di

Interest in the direct current effect on magnetoresistance in two-dimensional (2D) electron system (ES) has recently been revived due to the exciting experimental observations that in the case without irradiation, a relatively weak current can induce substantial magnetoresistance oscillations and negative differential resistivity.<sup>1,2,3,4</sup> Recent careful measurements<sup>5</sup> and theoretical analysis<sup>6</sup> disclosed accurate oscillating characteristic having the period  $\Delta\epsilon_j \sim 1$ , expressed by a dimensionless parameter  $\epsilon_j$  proportional to the ratio of the current density to the strength of the magnetic field.

The main oscillations appearing in the linear microwave photoresistance were known to be periodic in  $\epsilon_\omega = \omega/\omega_c$  ( $\omega$  is the angular frequency of the radiation and  $\omega_c = eB/m$  is the cyclotron frequency of an effective-mass  $m$  electron in the magnetic field  $B$ ), having the period  $\Delta\epsilon_\omega = 1$ .<sup>7,8,9,10,11,12,13,14,15,16,17,18,19,20</sup> Recent studies by Zhang *et al.*<sup>21</sup> on magneto-photoresistance in a 2DES subject to a microwave irradiation and a finite direct-current excitation revealed that the maxima (minima) of the differential resistance can evolve into minima (maxima) and back, and the oscillations are governed by a parameter  $\epsilon = \epsilon_\omega + \epsilon_j$ , combining the dc related parameter  $\epsilon_j$  and the radiation-frequency related parameter  $\epsilon_\omega$ .

The preliminary explanation of the observed resistance oscillations under simultaneous dc and ac excitations, which is based on indirect electron transitions consisting of a radiation-induced jump in energy and a dc-induced jump in space between Hall-field-tilted Landau levels,<sup>21</sup> is obviously not satisfied. A systematic theory capable of treating both excitations simultaneously within a single framework is highly desirable.

It is better to treat the magnetotransport subject to a strong dc excitation with a scheme direct using the electric current, rather than field, as the basic control parameter. Such a theory has been developed.<sup>15,19</sup> In this theory the integrative drift motion of the electron system opens new channels for individual electron to transit between different Landau levels through impurity and phonon scatterings, thus the direct current and the microwave radiation are dealt with on an equal footing.

We consider a 2DES having  $N_s$  electrons in a unit area of the  $x$ - $y$  plane subject to a uniform magnetic field  $\mathbf{B} = (0, 0, B)$  in the  $z$  direction. When an electromagnetic wave with incident electric field  $\mathbf{E}_{is} \sin \omega t$ , irradiates the 2D plane together with a dc electric field  $\mathbf{E}_0$  inside, the steady transport state of the system can be described by the electron drift velocity  $\mathbf{v}_0$  and an electron temperature  $T_e$ , satisfying the force and energy balance equations:<sup>19</sup>

$$N_s e \mathbf{E}_0 + N_s e (\mathbf{v}_0 \times \mathbf{B}) + \mathbf{F}_0 = 0, \quad (1)$$

$$N_s e \mathbf{E}_0 \cdot \mathbf{v}_0 + S_p - W = 0. \quad (2)$$

Here, the frictional force resisting electron drift motion,

$$\mathbf{F}_0 = \sum_{\mathbf{q}_{\parallel}} |U(\mathbf{q}_{\parallel})|^2 \sum_{n=-\infty}^{\infty} \mathbf{q}_{\parallel} J_n^2(\xi) \Pi_2(\mathbf{q}_{\parallel}, \omega_0 + n\omega), \quad (3)$$

is given by the electron density correlation function  $\Pi_2(\mathbf{q}_{\parallel}, \Omega)$ , the effective impurity potential  $U(\mathbf{q}_{\parallel})$ , a radiation-related coupling parameter  $\xi$  in the Bessel function  $J_n(\xi)$ , and  $\omega_0 \equiv \mathbf{q}_{\parallel} \cdot \mathbf{v}_0$ . The electron energy absorption from the radiation field,  $S_p$ , and the electron energy dissipation to the lattice,  $W$ , are given in Ref. 19. The nonlinear longitudinal resistivity and differential resistivity in the presence of a radiation field are direct obtained from Eq. (1) by taking  $\mathbf{v}_0$  (i.e the current  $\mathbf{J} = N_s e \mathbf{v}_0$ ) in the  $x$  direction,  $\mathbf{v}_0 = (v_0, 0, 0)$  and  $\mathbf{J} = (J, 0, 0)$ :

$$R_{xx} = -F_0 / (N_s^2 e^2 v_0), \quad (4)$$

$$r_{xx} = -(\partial F_0 / \partial v_0) / (N_s^2 e^2). \quad (5)$$

In the absence of microwave radiation, the formulation reduces to those presented in Ref. 6. The initial suppression and subsequent oscillation of the magnetoresistivity arise from the current-assisted electron transitions and are controlled by the parameter

$$\epsilon_j \equiv \frac{\omega_j}{\omega_c} = \frac{2mk_F v_0}{eB} = \sqrt{\frac{8\pi}{N_s}} \frac{m J}{e^2 B}. \quad (6)$$

The oscillating valley-peak pairs in the  $R_{xx}$ -vs- $\epsilon_j$  curve appear around the positions  $\epsilon_j = \eta m$  ( $m = 1, 2, \dots$ ), with

$\eta \sim 1$ , depending on the form of the scattering potential and on the electron temperature.

In the case of linear photoresistance,  $v_0 \rightarrow 0$ , the electron transition (intra- and inter-Landau levels) can take place by absorbing or emitting  $n$  photons of frequency  $\omega$  and jumping from Landau level  $l$  to  $l'$  (across  $m$  levels). This process gives rise to terms of  $\pm n$  in the frictional force  $\mathbf{F}_0$  expression Eq. (3). The periodicity of the electron density correlation function  $\Pi_2(\mathbf{q}_{\parallel}, \Omega + \omega_c) = \Pi_2(\mathbf{q}_{\parallel}, \Omega)$  at low electron temperature and many Landau-level occupation, leads to the appearance of peak-valley pairs in the linear magnetoresistivity around the positions of  $n\omega = m\omega_c$ .<sup>20</sup> The primary peak-valley pairs come from the single-photon process,  $n = 1$ , showing up around the node positions  $\omega = m\omega_c$ , or

$$\epsilon_{\omega} \equiv \omega/\omega_c = m = 1, 2, 3, \dots, \quad (7)$$

and the primary period of  $R_{xx}$  oscillation is  $\Delta\epsilon_{\omega} = 1$ . Two- and multiple-photon processes ( $n \geq 2$ ) yield secondary peak-valley pairs.<sup>20</sup>

When there is a finite bias current in 2DES, in view of the extra energy  $\omega_0 \equiv \mathbf{q}_{\parallel} \cdot \mathbf{v}_0$  provided by the electron drift motion together with the energy  $n\omega$  provided by the absorption or emission of  $n$  photons of the radiation field, an electron can be scattered by elastic impurities and jumps across  $m$  Landau levels of different energies. The resonance condition in this case should be determined by  $\eta\omega_j + n\omega = m\omega_c$ . Focusing only on single-photon processes ( $n = 1$ ), the valley-peak pairs of nonlinear magnetoresistance oscillations are anticipated to appear around the positions

$$\epsilon_{\omega} + \eta\epsilon_j = \epsilon_{\omega} (1 + \eta\omega_j/\omega) = m \quad (8)$$

or

$$\epsilon_{\omega} \equiv \omega/\omega_c = m/(1 + \gamma_j), \quad (9)$$

where  $m = 1, 2, 3, \dots$ , and

$$\gamma_j \equiv \eta\omega_j/\omega. \quad (10)$$

Therefore, the oscillating behavior of  $R_{xx}$  is controlled by the parameter  $\epsilon_{\omega} + \eta\epsilon_j$ , or  $\epsilon_{\omega}(1 + \gamma_j)$ .

Figure 1 presents the calculated longitudinal magnetoresistivity  $R_{xx}$  vs  $\epsilon_{\omega} = \omega/\omega_c$  for a GaAs-based 2DES with carrier density  $N_s = 3 \times 10^{15}/\text{m}^2$ , low-temperature linear mobility  $\mu_0 = 2000 \text{ m}^2/\text{Vs}$  at lattice temperature  $T = 1 \text{ K}$ , irradiated by a linearly  $x$ -direction polarized microwave of frequency  $\omega/2\pi = 100 \text{ GHz}$  and incident amplitude  $E_{is} = 5 \text{ V/cm}$ , and subject to bias velocities  $2v_0/v_F = 0, 0.001, 0.002, 0.003, 0.004, 0.005, 0.007, 0.01, 0.05$ , and  $0.1$  ( $v_F$  is the Fermi velocity), corresponding to current densities  $J = 0.06, 0.11, 0.17, 0.23, 0.29, 0.40, 0.57, 2.9$ , and  $5.7 \text{ A/m}$  or the bias parameter  $\omega_j/\omega = 0, 0.05, 0.1, 0.16, 0.21, 0.26, 0.36, 0.52, 2.6$ , and  $5.2$ , respectively. The elastic scatterings are assumed due to short-range impurities and the Landau level broadening

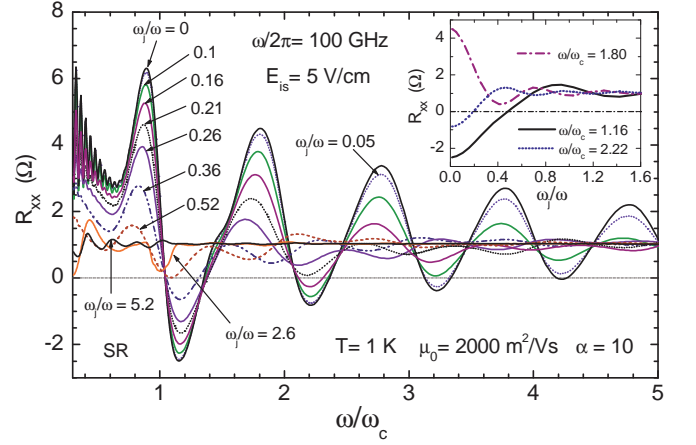


FIG. 1: (Color online) Longitudinal magnetoresistivity  $R_{xx}$  vs  $\epsilon_{\omega} = \omega/\omega_c$  for a GaAs-based 2DES with  $N_s = 3 \times 10^{15}/\text{m}^2$ ,  $\mu_0 = 2000 \text{ m}^2/\text{Vs}$  and  $\alpha = 10$  at lattice temperature  $T = 1 \text{ K}$ , under linearly polarized irradiation of frequency  $\omega/2\pi = 100 \text{ GHz}$  and incident amplitude  $E_{is} = 5 \text{ V/cm}$  and subject to bias current densities of  $\omega_j/\omega = 0, 0.05, 0.1, 0.16, 0.21, 0.26, 0.36, 0.52, 2.6$ , and  $5.2$ . The elastic scatterings are due to short-range impurities. The inset shows  $R_{xx}$  as a function of  $\omega_j/\omega$  at three fixed magnetic field strengths,  $\omega/\omega_c = 1.16, 1.80$ , and  $2.22$ .

parameter is taken to be  $\alpha = 10$ .<sup>19</sup> Linear (zero dc bias,  $\omega_j = 0$ ) magnetoresistivity exhibits typical feature of radiation-induced magnetoresistance oscillations, with two-photon process slightly showing up as a shoulder around  $\epsilon_{\omega} \approx 1.5$ . In the case of small dc bias,  $\gamma_j \ll 1$ , the node positions of peak-valley pairs are shifted down from  $\epsilon_{\omega} = m$  at zero dc bias to  $\epsilon_{\omega} = m/(1 + \gamma_j) \approx m - m\gamma_j$ . The shifted distances relative to the original positions,  $m\gamma_j$ , are larger for larger  $m$ , but still locate within the same order of  $\epsilon_{\omega}$  as long as  $m\gamma_j < 1$ . When the shifted distance becomes as large as 0.5, the original peak will move to the range where previously there is a valley. In the case of strong dc bias,  $\gamma_j > 1$ , the original pairs of higher order (larger  $m$ ) may shift to lower order range of  $\epsilon_{\omega}$ . For instance, in the case of short-range impurity scattering  $\eta = 0.94$ ,<sup>6</sup> for the bias current of  $\omega_j/\omega = 5.2$  ( $\gamma_j = 4.9$ ), the original pairs at  $\epsilon_{\omega} = m$  with  $m = 1, 2, 3, 4, 5$ , and  $6$  are shifted to the positions  $\epsilon_{\omega} = m/(1 + \gamma_j) = 0.17, 0.34, 0.51, 0.68, 0.85$ , and  $1.02$ . Except for the first one ( $\epsilon_{\omega} = 0.17$ ), which is beyond the range plotted, the other five pairs are clearly identified in the figure.

The inset of Fig.1 shows the change of the magnetoresistivity  $R_{xx}$  with increasing bias current density  $J$  in terms of  $\omega_j/\omega$  at three fixed magnetic field strengths  $\omega/\omega_c = 1.16, 1.80$ , and  $2.22$ , respectively, near the first minimum, the second maximum and minimum of  $R_{xx}$ . Here we show the fact that within a certain magnetic field range of resistivity minimum,  $R_{xx}$  can be negative at small  $J$  but increases with increasing  $J$  and passes through zero at a finite  $J$ .<sup>15</sup> This is exactly what is re-

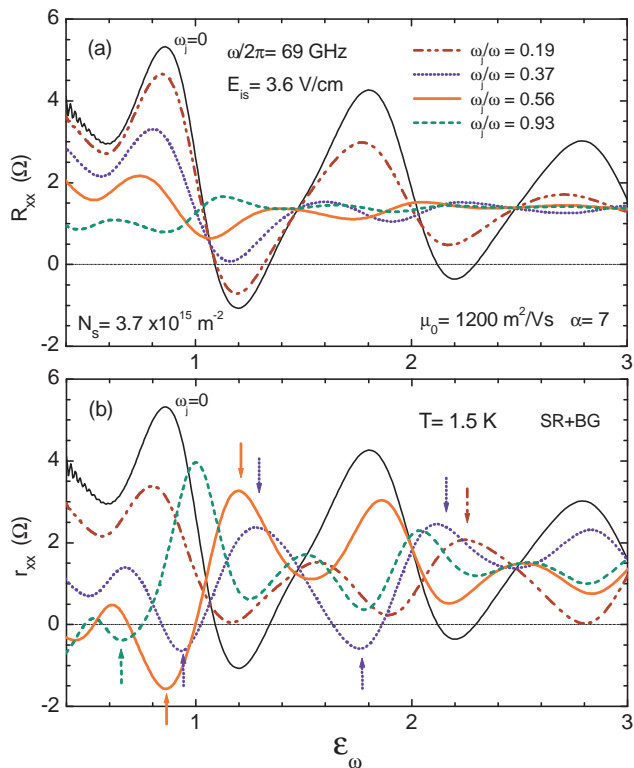


FIG. 2: (Color online) Longitudinal magnetoresistivity  $R_{xx}$  (a) and differential magnetoresistivity  $r_{xx}$  (b) vs  $\epsilon_\omega \equiv \omega/\omega_c$  for a GaAs-based 2DES with  $N_s = 3.7 \times 10^{15}/\text{m}^2$  and  $\mu_0 = 1200 \text{ m}^2/\text{Vs}$  at  $T = 1.5 \text{ K}$ , under irradiation of a linearly polarized microwave of frequency  $\omega/2\pi = 69 \text{ GHz}$  and incident amplitude  $E_{is} = 3.6 \text{ V/cm}$ , and subject to bias current densities of  $\omega_j/\omega = 0, 0.19, 0.37, 0.56,$  and  $0.93$ . The elastic scatterings are from a mixture of short-range (SR) and background (BG) impurities.

quired for the instability of the time-independent small-current solution and for the development of a spatially nonuniform<sup>22,23</sup> or a time-dependent state,<sup>24</sup> which exhibits measured zero resistance. Therefore, the region where an absolute negative dissipative magnetoresistance develops is identified as that of zero-resistance state.

The calculated longitudinal magnetoresistivity  $R_{xx}$  and differential magnetoresistivity  $r_{xx}$  for another GaAs-based 2DES with carrier density  $N_s = 3.7 \times 10^{15}/\text{m}^2$  and low-temperature linear mobility  $\mu_0 = 1200 \text{ m}^2/\text{Vs}$  at lattice temperature  $T = 1.5 \text{ K}$  are plotted in Fig. 2 as functions of  $\epsilon_\omega \equiv \omega/\omega_c$ , under the irradiation of a linearly  $x$ -direction polarized microwave of frequency  $\omega/2\pi = 69 \text{ GHz}$  with incident amplitude  $E_{is} = 3.6 \text{ V/cm}$ , and subjected to bias drift velocities  $2v_0/v_F = 0, .002, .004, .006,$  and  $0.01$ , corresponding to current densities  $J = 0, 0.14, 0.28, 0.42,$  and  $0.70 \text{ A/m}$  or bias parameter  $\omega_j/\omega = 0, 0.19, 0.37, 0.56,$  and  $0.93$ , respectively. The elastic scatterings are assumed due to a mixture of short-range and background impurities and the broadening parameter is taken to be  $\alpha = 7$ . We see that positions of peak-valley pairs and their maxima and min-

ima of different  $\epsilon_\omega$  orders  $m$  in the zero-bias  $R_{xx}$  curves [Fig. 2(a)] are shifted downward with increasing current density  $\omega_j/\omega$  following the same rule as stated in the case of Fig. 1.

The oscillations of differential resistivity  $r_{xx}$  exhibit shorter period and much larger amplitude than those of  $R_{xx}$ , especially at high dc bias where  $R_{xx}$  oscillations become less prominent, as shown in Fig. 2(b). Positions of peak-valley pairs and their maxima and minima in  $r_{xx}$  are shifted downward further relative to those of the corresponding  $R_{xx}$  at the same order  $m$ . Of particular interest is that with increasing bias current density, in the  $\epsilon_\omega$  range where the zero-bias magnetoresistivity ( $R_{xx} = r_{xx}$ ) exhibits positive maximum, the differential magnetoresistivity  $r_{xx}$  can be driven down to a considerable negative value, as indicated by the up-directed arrows in Fig. 2(b); and in the  $\epsilon_\omega$  range where the zero-bias magnetoresistivity ( $R_{xx} = r_{xx}$ ) exhibits a minimum, the differential magnetoresistivity  $r_{xx}$  can be driven up to exhibit a maximum, as indicated by the down-directed arrows in Fig. 2(b).

According to electrodynamic analyses, a homogeneous state of current  $J$  is unstable if either the absolute dissipative resistivity  $R_{xx}$  or the differential resistivity  $r_{xx}$  becomes negative.<sup>22,23</sup> Thus, despite the detailed structure yet to be explored, it is expected that, under appropriate conditions, a zero-resistance state (ZRS) or some kind of quasi-ZRS could be measured in the region where  $R_{xx}$  or  $r_{xx}$  exhibits a negative value in a homogeneous microscopic analysis. With this in mind, the  $R_{xx}$  and  $r_{xx}$  behaviors in Fig. 2 could predict the following measured results. In the vicinity around  $\epsilon_\omega = 2.25$ , the ZRS showing up in the zero dc bias will disappear at bias  $\omega_j/\omega \geq 0.10$  because both  $R_{xx}$  and  $r_{xx}$  return to positive. Instead, one should observe a bulged  $r_{xx}$  in the cases of  $\omega_j/\omega = 0.19, 0.37,$  and  $0.93$  and a dented  $r_{xx}$  in the case of  $\omega_j/\omega = 0.56$ , as shown in Fig. 2. In the vicinity around  $\epsilon_\omega = 1.25$ , where the negative  $R_{xx}$  (thus the ZRS) maintains up to the dc bias  $\omega_j/\omega = 0.35$ , one may not detect  $r_{xx}$  significantly different from zero at low dc biases but the bulged  $r_{xx}$  should be observed at higher dc biases when  $R_{xx}$  becomes positive and the ZRS disappears, as seen in Fig. 2 in the cases of  $\omega_j/\omega = 0.37$  and  $0.56$ . In the vicinity around  $\epsilon_\omega = 1.75$  and  $0.8$ , the zero-bias magnetoresistivity  $R_{xx} = r_{xx}$  exhibits main peaks while the differential resistivity  $r_{xx}$  becomes negative, respectively, at finite dc biases  $\omega_j/\omega = 0.37$  and  $0.56$ , suggesting the possible ZRS induced by the direct current. When further increasing current density, it disappears and becomes a bulged differential resistivity. In the range  $0.6 \leq \epsilon_\omega \leq 1$  the differential resistivity  $r_{xx}$  at all three strong dc biases ( $\omega_j/\omega = 0.37, 0.56,$  and  $0.93$ ) can become negative, implying possible resistance suppression or quasi-ZRSs induced by the bias current. These results indeed show up in a recent experimental observation.<sup>21</sup>

This work was supported by the projects of the National Science Foundation of China, the special Funds for Major State Basic Research Project, and the Shang-

- 
- <sup>1</sup> C. L. Yang, J. Zhang, R. R. Du, J. A. Simmons, and J. L. Reno, *Phys. Rev. Lett.* **89**, 076801 (2002).
- <sup>2</sup> R. G. Mani, V. Narayanamurti, K. von Klitzing, J. H. Smet, W. B. Johnson, and V. Umansky, *Phys. Rev. B* **70**, 155310 (2004).
- <sup>3</sup> A. A. Bykov, J. Q. Zhang, S. Vitkalov, A. K. Kalagin, and A. K. Bakarov, *Phys. Rev. B* **72**, 245307 (2005).
- <sup>4</sup> J. Q. Zhang, S. Vitkalov, A. A. Bykov, A. K. Kalagin, and A. K. Bakarov, *Phys. Rev. B* **75**, 081305 (2007).
- <sup>5</sup> W. Zhang, H. -S. Chiang, M. A. Zudov, L. N. Pfeiffer, and K. W. West, *Phys. Rev. B* **75**, 041304 (2007).
- <sup>6</sup> X. L. Lei, *Appl. Phys. Lett.* **90**, 132119 (2007).
- <sup>7</sup> V. I. Ryzhii, *Sov. Phys. Solid State* **11**, 2087 (1970).
- <sup>8</sup> M. A. Zudov, R. R. Du, J. A. Simmons, and J. L. Reno, *Phys. Rev. B* **64**, 201311(R) (2001).
- <sup>9</sup> P. D. Ye, L. W. Engel, D. C. Tsui, J. A. Simmons, J. R. Wendt, G. A. Vawter, and J. L. Reno, *Appl. Phys. Lett.* **79**, 2193 (2001).
- <sup>10</sup> R. G. Mani, J. H. Smet, K. von Klitzing, V. Narayanamurti, W. B. Johnson, and V. Umansky, *Nature* **420**, 646 (2002); *Phys. Rev. Lett.* **92**, 146801 (2004).
- <sup>11</sup> M. A. Zudov, R. R. Du, L. N. Pfeiffer, and K. W. West, *Phys. Rev. Lett.* **90**, 046807 (2003).
- <sup>12</sup> S. I. Dorozhkin, *JETP Lett.* **77**, 577 (2003).
- <sup>13</sup> R. L. Willett, L. N. Pfeiffer, and K. W. West, *Phys. Rev. Lett.* **93**, 026804 (2004).
- <sup>14</sup> A. C. Durst, S. Sachdev, N. Read, and S. M. Girvin, *Phys. Rev. Lett.* **91**, 086803 (2003).
- <sup>15</sup> X. L. Lei and S. Y. Liu, *Phys. Rev. Lett.* **91**, 226805 (2003); X. L. Lei, *J. Phys.: Condens. Matter* **16**, 4045 (2004).
- <sup>16</sup> I. A. Dmitriev, A. D. Mirlin, and D. G. Polyakov, *Phys. Rev. B* **69**, 035303 (2004).
- <sup>17</sup> V. I. Ryzhii and R. Suris, *J. Phys.: Condens. Matter* **15** (2003).
- <sup>18</sup> M. G. Vavilov and I. L. Aleiner, *Phys. Rev. B* **69**, 035303 (2004).
- <sup>19</sup> X. L. Lei and S. Y. Liu, *Phys. Rev. B* **72**, 075345 (2005).
- <sup>20</sup> X. L. Lei and S. Y. Liu, *Appl. Phys. Lett.* **88**, 212109 (2006).
- <sup>21</sup> W. Zhang, M. A. Zudov, L. N. Pfeiffer, and K. W. West, *Phys. Rev. Lett.* **98**, 106804 (2007).
- <sup>22</sup> A. V. Andreev, I. L. Aleiner, and A. J. Mills, *Phys. Rev. Lett.* **91**, 056803 (2003).
- <sup>23</sup> J. Alicea, L. Balents, M. P. A. Fisher, A. Paramekanti, and L. Radzihovsky, *Phys. Rev. B* **71**, 235322 (2005).
- <sup>24</sup> T. K. Ng and Lixin Dai, *Phys. Rev. B* **72**, 235333 (2005).